Newly identified uranyl vanadate mineral formation in the Thrace Basin, NW Türkiye: Insights into identification and origin of carnotite and tyuyamunite minerals

Ebru SEZEN[a]* and Zehra S. KARAKAŞ[b]

[a] General Directorate of Mineral Research and Exploration (MTA), Department of Energy Raw Material Research and Exploration, Ankara, Türkiye. 0009-0009-2442-9286

[b] Ankara University, Faculty of Engineering, Department of Geological Engineering, Ankara, Türkiye 0000-0002-5620-4518

**Corresponding author: Ebru SEZEN, ebru.sezen@mta.gov.tr*

ABSTRACT

The Thrace Basin is located in the northwest of Türkiye, bounded by the Rhodope Zones to the west, the Strandja (Istranca, Strandzha) Massif to the North, and the İstanbul Zone to the east. The Stranja Massif's basement is composed of the Tekedere Group, which includes Paleozoic gneisses and schists, as well as the Şeytandere Metagranite, consisting of altered and unaltered metagranites. Unaltered metagranites are characterized by large feldspar crystals and are typically white and pink in color, while altered metagranites are typically yellow color. The subject of this study Şeytandere metagranites which the uraninite mineral, for the first time, was identified in unaltered metagranite samples, while carnotite and tyuyamunite minerals were identified in altered meta-granite samples. The morphologies and elemental compositions of these minerals were identified by Scanning Electron Microscopy (SEM) and Energy Dispersive X-ray Spectroscopy (EDS). The SEM-EDS analyses revealed that the major elements of carnotite [$K_2(UO_2)_2(V_2O_8)(H_2O)_3$] and tyuyamunite [$Ca(UO_2)_2(V_2O_8)(H_2O)_8$] are of K, U and V and Ca, U and V, respectively. In the investigated samples carnotite has a plate-like morphology, whereas tyuyamunite shows a fibrous apperance. This investigation shows that carnotite and tyuyamunite are epigentically formed from uranyl vanadate minerals in the Şeytandere metagranite. These minerals indicate uranium leaching from granitic materials and re-deposition as fine specks in open pores by circulating meteoric water. The leached uranyl ions, combined with vanadate ions, form carnotite and tyuyamunite under weathering conditions.

Keywords: Uranium, Carnotite, Tyuyamunite, Şeytandere Metagranite, Thrace Basin, Türkiye.

1.Introduction

In the world, the exploration of radioactive elements is of significant importance for supplying raw materials to nuclear power plants. The primary raw material sources for nuclear energy are the elements uranium and thorium. The main uranium minerals that form economically significant deposits in nature are uraninite, pitchblende, torbernite, metatorbernite, coffinite, autunite, metaautunite, bassetite, phosphuranylite, and uranophane. Additionally, uranyl vanadate minerals such as carnotite [$K_2(UO_2)_2(V_2O_8)$ $(H_2O)_3$] and tyuyamunite [$Ca(UO_2)_2(V_2O_8)(H_2O)_8$] are abundant and significant components of many uranium deposits (Stern et al., 1956; Frondel, 1958; Evans and White, 1987; Avasarala et al., 2020; Glasauer et al. 2022). These minerals are often important for uranium mining and nuclear fuel production and are found in several geological settings around the world.

Carnotite and tyuyamunite are secondary uranyl vanadate minerals that often form together and are found in similar geological environments. These mineral formations have been determined in regions of the world such as the Colorado Plateau (Hillebrand, 1924; Weeks and Thompson, 1954; Stern et al., 1956; Wenrich-Verbeek et al., 1982; Finch and Davis, 1985), Sonora, Texas (Onac et al., 2001), South Dakota, Arizona, Utah, Pennsylvania (Hillebrand, 1924; Stokes, 1944; Sharma et al., 2016; Blake et al., 2015, 2019), the Saskatchewan region of Canada (Langford, 1974), New Mexico (Burillo et al., 2012; Caldwell, 2018), Queensland and South Australia (Crook and Blake, 1910; Parkin and Glasson, 1954), in China (Xu et al., 2015), near Kokand and Fergana in eastern Uzbekistan, Kazakhstan, the Congo, Morocco, and in some uranium mines in Namibia and Egypt (Hassan et al., 1983; Bowell and Davies, 2017; Gheith et al., 2018; Hamza et al., 2020).

Uranium exploration in the Thrace Basin was carried out in the form of aerial and ground radiometric studies between 1975 and 1979 (Sungur 1976, 1980). These studies identified anomalies in the Istranca Massif and Eocene-aged tuffitic sandstones. Geological mapping, scintillometry studies, stream sediment studies, water sampling for uranium and radon, radon measurement in soil, coreless drilling, and radiometric determinations were conducted in the basin (Denkel, 1956, 1957; Denkel and Taşdemiroğlu 1956; Taşdemiroğlu, 1958, Yavaş, 1959a, b, Uncugil 1968, Acar 1969, Yılmaz 1969, Sungur 1976, 1980; Küçük, 2018; Sezen and Taşkıran, 2020; Çelikkurt, 2020; Tunç et al., 2024). Uranium content has been identified in the sandstone and claystone beds of the Oligocene-aged Süloğlu Formation in the Edirne-Havsa region of the Thrace Basin, NW Türkiye (Sezen and Taşkıran, 2020).

Newly identified carnotite and tyuyamunite formations have, for the first time, been recorded in the Thrace Basin, which is significant for discussions on uranium prospecting and the origin of secondary uranium deposits

(Figure 1). Therefore, the purpose of this study focuses on the morphology and elemental composition of carnotite and tyuyamunite minerals using some analytical techniques such as Scanning Electron Microscope (SEM) and Energy Dispersive Spectroscopy (EDS) analysis, and X-Ray Powder Diffractometer (XRD) analyses.

2. Geology

The Thrace Basin is a Tertiary basin bounded by Greece, Bulgaria and the Rhodope Zones to the west; the Strandja Massif, Bulgaria and the Black Sea to the North; part of the Marmara Sea and the Istanbul Zone to the east; and the Marmara Sea, the Dardanelles, the Saroz Gulf and the northern part of the Aegean Sea to the South (Figure 1). The Thrace Basin is characterized by the Rhodope Zone, the Istanbul Zone, and the metamorphic rocks of the Istranca Massif, which are overlaid by Tertiary-aged cover units in the southwest of the massif (Okay and Yurtsever, 2006; Okay et al., 2001). The Rhodope zone is represented by ultramafic rocks, phyllites, metasediments, gneisses and micaschists. The Istanbul Zone consists of sandstones, limestones and siltstones.

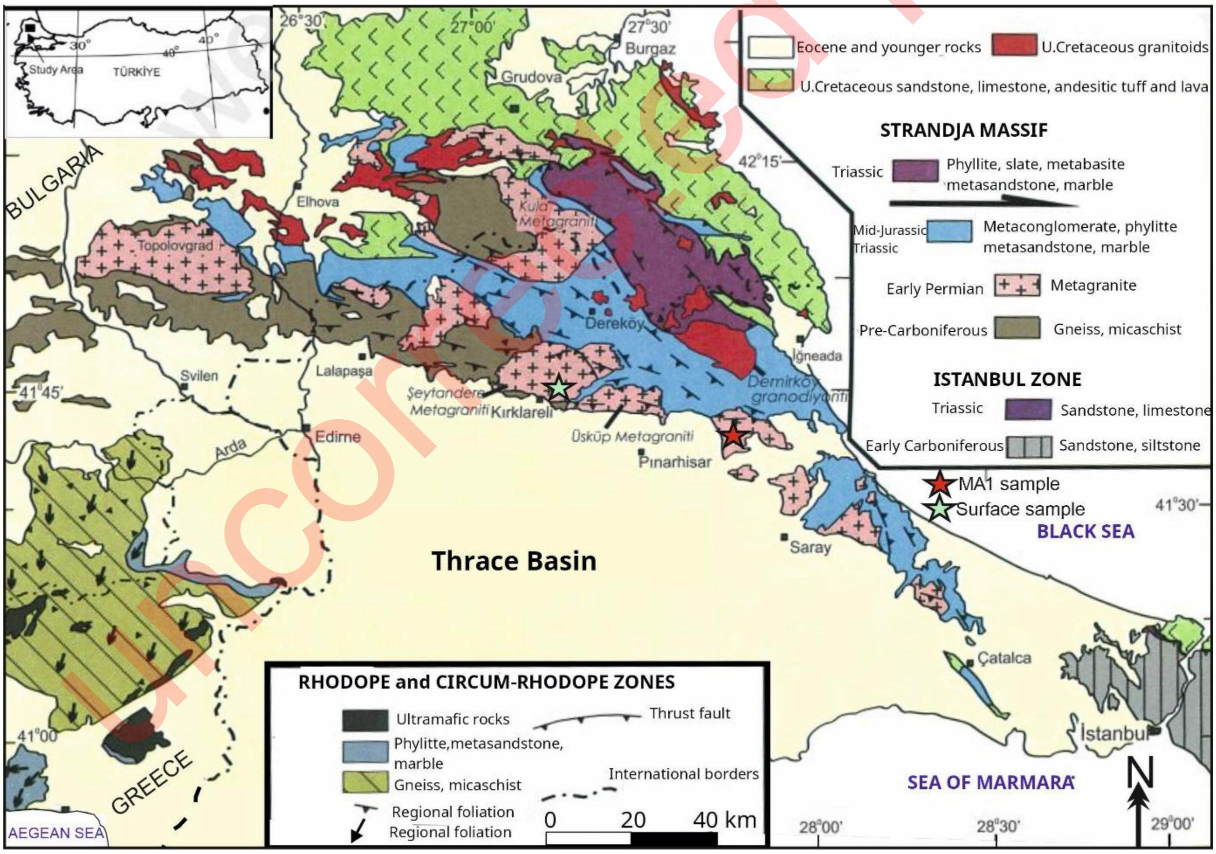

Figure 1 Simplified geological map of the study area (modified from Okay et al., 2001) and the sample locations (S and MA-1) .

The Stranja Massif consists of gneiss, micaschist, metagranite, metaconglomerate, phyllite, metasandstone and marble units (Okay et al., 2001). In the study area, the Tekedere Group, represented by schists and gneisses, is cut by the Şeytandere metagranites belonging to the Kırklareli Group (Figure 2).

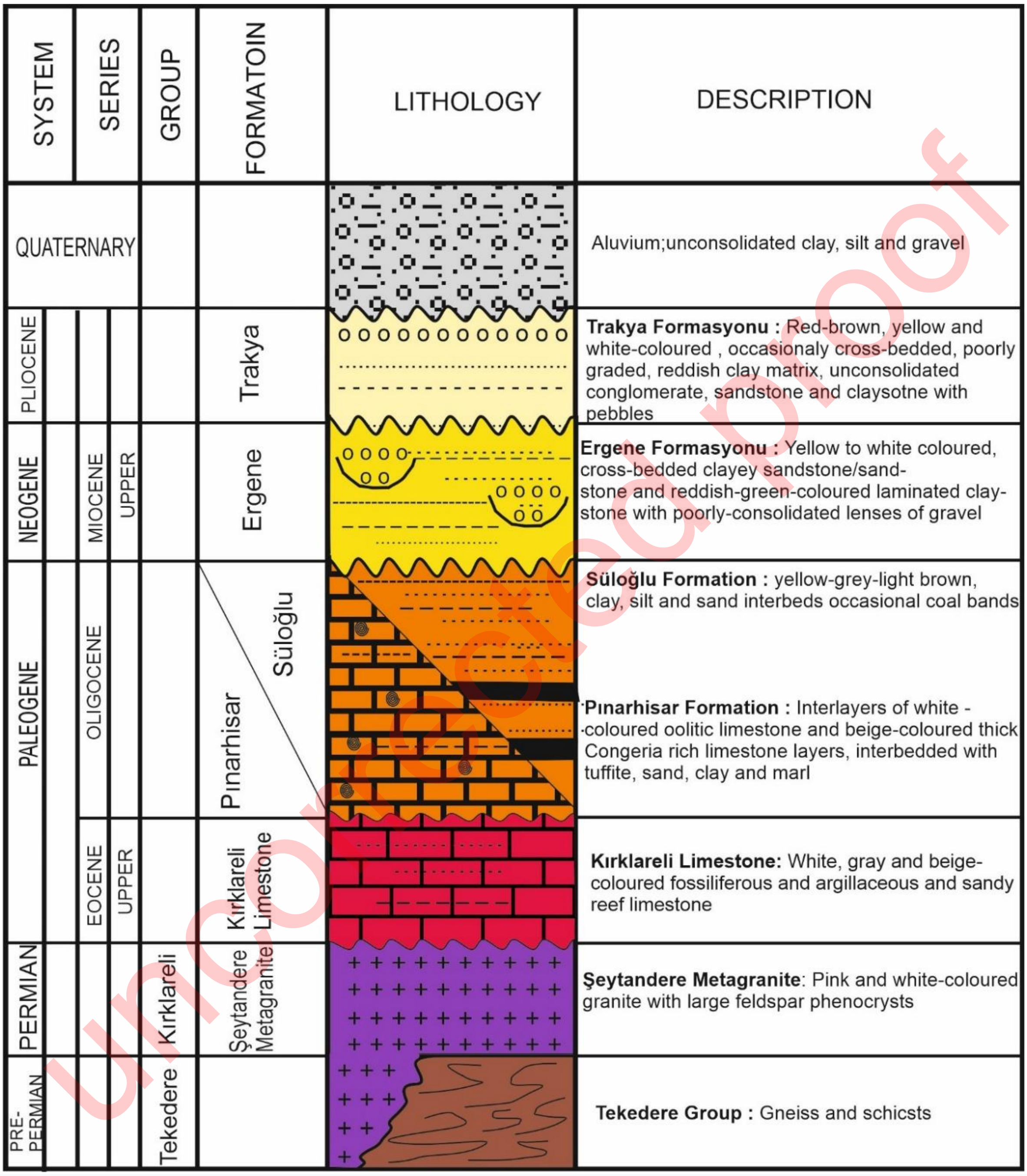

Figure 2. Generalized stratigraphic section of the study area, modified from Sezen and Taşkıran (2020) and see also Çağlayan and Yurtsever (1998).

The Şeytandere Metagranite mainly comprises pink and white metagranites containing large feldspar phenocrysts (Çağlayan and Yurtsever, 1998). Altered metagranite samples are typically characterized by their yellow color appearance in the field.

The Tertiary sediments of the Thrace basin, according to the studies of Çağlayan and Yurtsever (1998), begin with the Eocene-aged İslambeyli Formation with, beige-white volcanic clastics, sandy and clayey limestone, sandstone, and marl (Figure 2). Outcrops of this unit are not observed in the study area. The İslambeyli Formation is overlain by the late Eocene-aged Kırklareli Limestone, which is represented by white, sometimes yellow, abundant fossiliferous sandy and clayey reef limestones. These units are unconformably overlain by the Pınarhisar Formation, which consists of Oligocene-aged white-colored oolitic limestone and beige-colored, thick-layered limestone with abundant congeria, tuffite, sand, and clay marl interlayers. The Süloğlu Formation conformably overlies the Pınarhisar Formation. The Süloğlu Formation corresponds to the upper levels of lignite and sandstones, which are defined as the Danişmen Formation in the region (Şafak ve Güldürek 2016). This formation is composed of alternating layers of sandstone, siltstone, and claystone with, lignite and uranium deposits. It is characterized by its yellow, grey, and light brown colors, with coal bands in places. These units are unconformably overlain by the Ergene Formation, which consists of yellowish-white and white cross-bedded clayey sandstone and light green laminated claystone from the late Miocene. The Trakya Formation, which consists of yellowish-brown, red, and yellowish-white colored cemented/unconsolidated gravel, sand, and mudstone and covers a large area in the study area, is Pliocene in age. Quaternary alluvium covers all these units with angular unconformity, especially in the stream beds.

3. Material and Method

During the study, twenty-five samples were collected from the Seytandere metagranites, which are thought to be the source rock of uranium. Ten of these are altered rock samples taken from the surface, and fifteen are unaltered core samples taken from drill hole MA-1 (Figure 1). The XRD method was used to determine the mineral compositions of four samples, which contained uranium in concentrations ranging from 136,8 ppm to 8489,5 ppm, as well as the uranium minerals that contribute to uranium mineralization. The whole-rock XRD analysis of the samples was conducted in the laboratories of the Mineral Research and Exploration General Directorate (MTA), Mineral Analysis and Technology (MAT) Department. A Panalytical X Pert Powder model X-Ray Diffractometer with a Copper (Cu) tube was used for the XRD analysis of the powdered samples.

The whole-rock analyses were conducted within the range of 4°-70° 2Θ. The American Standard for Testing Material (ASTM 1972) catalog was used for the evaluation of the diffractograms. After identifying all rock components through XRD analysis, their semi-quantitative percentages were calculated based on the external standard method (Brindley, 1980; Gündoğdu, 1982). The morphology of the minerals constituting the uranium anomaly and their textural relationships with other minerals were examined using the Scanning Electron Microscope (SEM) method. The samples to be examined by SEM were coated with gold and prepared for analysis. SEM-EDS analysis was performed on samples that showed anomaly values above 900-3000 cps in radioactivity measurements made with scintillometer and gamma ray spectrometer devices. To obtain better SEM images, considering the atomic number of the uranium element, images were taken using a backscattered electron (BSE) detector. The point chemical compositions of the minerals were attempted to be determined using Energy Dispersive X-ray Spectroscopy (EDAX/EDS) analysis. The examinations were carried out with the FEI Quanta 400 device in the technology laboratories of the MAT department at MTA.

4. Results and discussion

4.1. X-Ray Diffraction (XRD) Analyses

The mineralogical compositions of the rock samples taken from the Şeytandere Metagranites were studied by XRD analyses to identify the type of uranium mineral(s) responsible for the observed uranium mineralization in these samples. However, the identification of peaks characteristic of uranium minerals presented challenges during XRD examinations due to their concentration. Specifically, the low concentration of uranium minerals in the samples prevented the observation of their strong characteristic peaks. Additionally, the presence of strong peaks from minerals such as quartz and feldspar further complicated the identification of uranium mineral peaks.

Quartz was the most commonly observed silicate mineral in the samples, accompanied by feldspar minerals in varying amounts (Table 1). Quartz was identified by its peaks at 4.26 Å, 3.34 Å, 2.45 Å, and 2.27 Å; feldspar by its peaks at 3.25 Å and 3.21-3.18 Å and 2.92 Å (Figures 3, 4). Additionally, mica with peaks at 10.00 Å and 4.99 Å, as well as a clay mineral with peaks at 7.18 Å and 3.58 Å, were identified in the unaltered metagranite samples. The clay mineral was likely formed by the alteration of feldspars. Quartz, feldspar, and mica constitute the main mineral composition of the granite rock.

According to XRD analysis, the peaks observed at 3.14 Å, 2.73 Å, and 1.93 Å were attributed to uraninite (UO_2), consistent with the findings of Smith et al. (2010), who reported similar peak positions in their study of uranium-bearing formations (Figure 3). Additionally, peaks at 6.56 Å, 4.26 Å, and 3.12 Å were identified as carnotite (K2(UO2)2(VO4)2·3H2O), corroborating the results reported by Johnson and Blake (2015) in their comprehensive analysis of vanadium-uranium deposits (Figures 4).

Table 1. XRD results of Şeydandere Metagranite samples

Sample Number	MA1-10	MA1-11	U-4	U-5
Sample Type	Drill core Samples		Surface Samples	
Lithology	Unaltered Metagranite		Altered Metagranite	
U (ppm)	136,8	458,8	8489,5	749,5
Qz	X	X	X	X
Fsp	X	X	X	X
Cal			X	X
Mic	X	X		
Clm	X	X		
Urn	X	X		
Crn			X	X

(Qz: quartz, Fsp: feldspar, Cal: calcite, Mic: Mica, Clm; Clay Mineral, Urn: uraninite, Crn: Carnotite). Abbreviations after Whitney and Evans (2010).

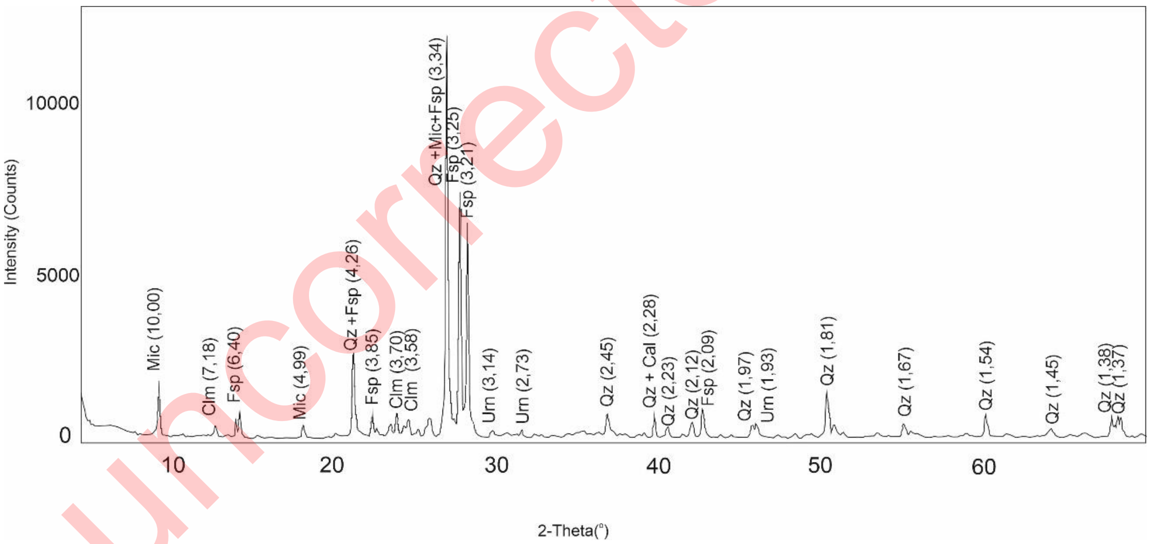

Figure 3. XRD diffractogram of unaltered granite sample MA1/11 (Qz: quartz, Fsp: feldspar, Mic: Mica, Clm: Clay Mineral, Urn: uraninite. Abbreviations after Whitney and Evans, 2010)

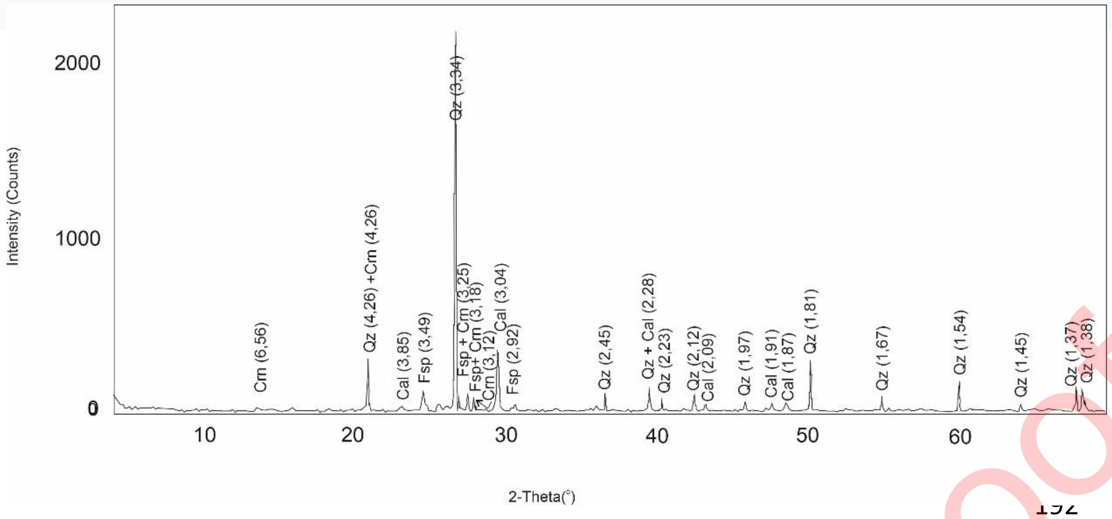

Figure 4. XRD diffractogram of altered granite sample U-4 (Qz: quartz, Fsp: feldspar, Cal: calcite, Crn: Carnotite. Abbreviations after Whitney and Evans, 2010)

The uraninite mineral was identified in unaltered drill core samples, while the carnotite mineral was identified in altered metagranites in surface samples. The main mineral composition of the altered metagranite samples consists of quartz, feldspar, and calcite minerals. The calcite, which was detected in the altered samples but not in the unaltered ones, was likely formed through carbonation-type alteration. Mica and clay minerals were not detected in the altered metagranite samples.

4.2. Scanning Electron Microscope (SEM-EDS) Determinations

SEM analyses revealed that the very-white structures, approximately 60 µm in size, were identified as uranium-bearing minerals (Figures 5, 6). In the EDS analysis results, K, U, and V were determined as the main elements forming the Carnotite mineral [$K_2(UO_2)_2(V_2O_8)$ $(H_2O)_3$]composition (Figure 5g). A similar major element composition has also been identified in studies conducted by Gheith et al. (2018), Hamza et al. (2020), Nasr (2021), and Frankland et al. (2022). Carnotite mineral, determined as a mono-mineral aggregate, has a plate-like morphology (Figures 5a-f). Frankland et al. (2022) stated that the platy micromorphology of the crystallites is consistent with Carnotite’s perfect 'micaceous' basal [001] cleavage. The main elemental components of the tyuyamunite mineral [$Ca(UO_2)_2(V_2O_8)(H_2O)_8$] were Ca, U, and V (Figures 6b and 6e). Tyuyamunite mineral was observed in fibrous form among the grains. The morphological characteristics and major element compositions of the tyuyamunite mineral identified alongside the carnotite mineral are similar to those reported in studies by Gheith et al. (2018), Nasr (2021), and Frankland et al. (2022). The Si and Al elements observed in the EDS spectra were attributed to the presence of quartz and aluminous silicate minerals in the samples.

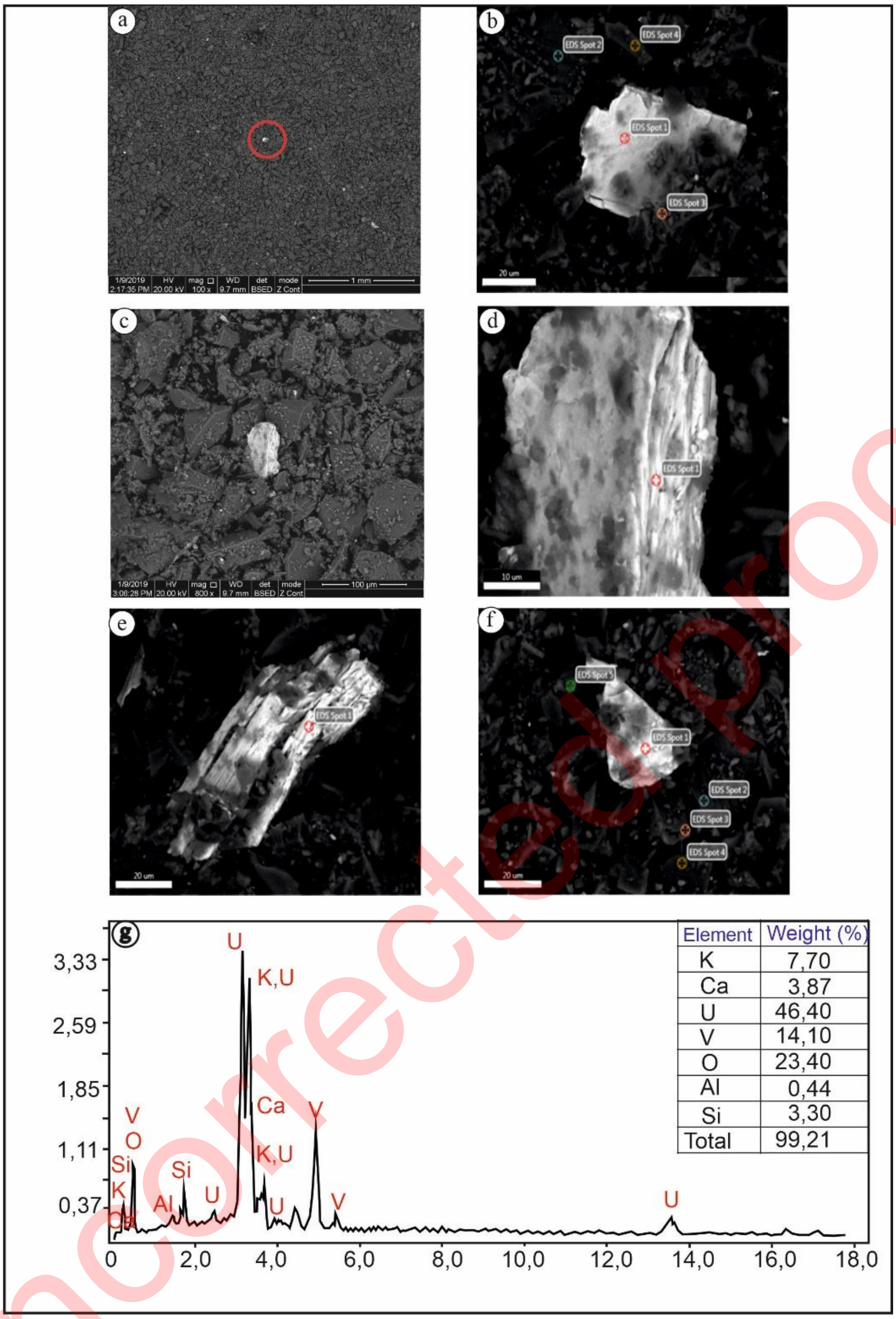

Figure 5. SEM photomicrographs of carnotite fragments (a) SEM-BSE image of fragments of very fine, monomineralic carnotite. (b) A close view of the Carnotite, (c) SEM-BSE image of fragments of very fine, monomineralic carnotite. (d) A close view of the Carnotite, (e, f)) SEM-BSE image of carnotit, (g) EDS spectrum from a typical carnotite fragment.

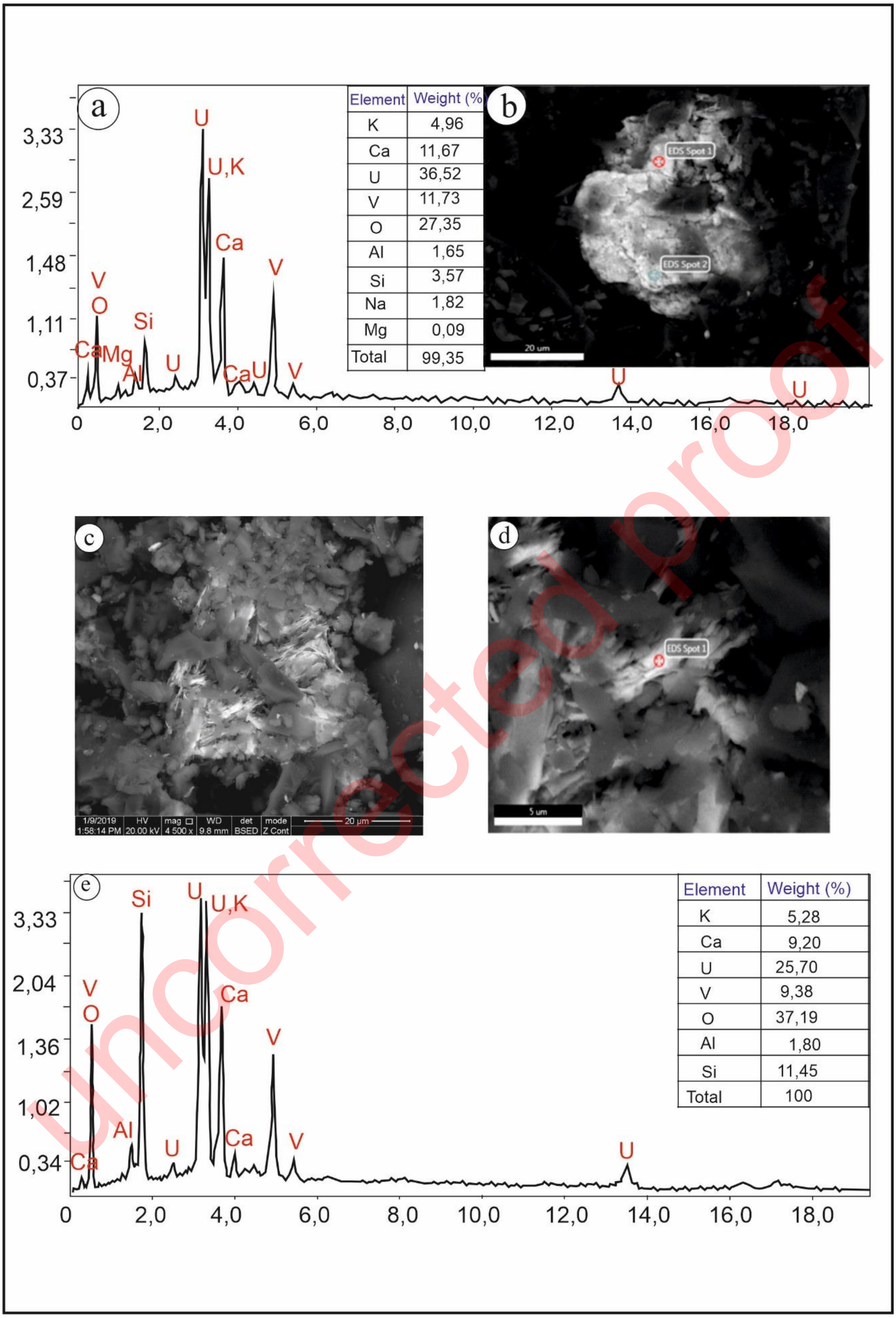

Figure 6. SEM photomicrographs of tyuyamunite crystals (a) SEM-BSE image of tyuyamunite. (b) EDS spectrum from a typical tyuyamunite fragment, (c, d) A close view of fibrous tyuyamunite crystal morphology, (e) EDS spectrum from a typical tyuyamunite fragment.

5. Discussion

In this study, secondary-formed carnotite [$K_2(UO_2)_2(V_2O_8)(H_2O)_3$] and tyuyamunite [$Ca(UO_2)_2(V_2O_8)(H_2O)_8$] mineral associations were identified in altered surface samples of the Şeytandere metagranites in the Thrace Basin. Additionally, uraninite was detected in unaltered Şeytandere metagranite samples. Similarly, carnotite, tyuyamunite, and/or meta-tyuyamunite, which are secondary-formed uranyl vanadate minerals, are commonly found together in uranium deposits (Stern et al., 1956; Frondel, 1958; Wenrich-Verbeek et al., 1982; Evans and White, 1987; Onac et al., 2001; Avasarala et al., 2020; Glasauer et al., 2022). The formation of carnotite and tyuyamunite minerals in the Thrace Basin was primarily influenced by uranium sourced from acidic intrusive rocks, specifically the Şeytandere metagranites. Likewise, Nakoman (1978) identified acidic granites, alkaline complexes, and felsic rocks as primary host rocks for uranium in the Earth's crust. Furthermore, Sezen and Taşkıran (2020) suggested that acidic magmatic rocks in the Thrace Basin could serve as source rocks for uranium.

The Şeytandere metagranites have contributed to the formation of various types of radioactive mineral deposits through different processes, either directly or indirectly, in the region. In addition to quartz, feldspar, and mica, which constitute the main mineral composition of metagranites as determined by XRD analyses, secondary minerals such as zircon, sphene, and monazite, containing radioactive elements below 1% of the mineral composition of these rocks, are the main sources of uraninite. Uranium concentrations of 136.8 ppm and 458.8 ppm, determined in unaltered Şeytandere metagranite drilling samples, along with the presence of uraninite identified by small peaks in XRD analyses, support this view (Table 1, Figure 3). Various studies have noted that primary uranium minerals, such as uraninite and coffinite, which have a valence of 4, are found in granite rocks (Kaplan,1978; Nakoman, 1978).

Uraninite found in the Şeytandere metagranites is primary and stable but has transformed into secondary uranium minerals, such as carnotite and tyuyamunite, under oxidizing conditions. The formation of carnotite and tyuyamunite minerals has been significantly influenced by the alteration of the Şeytandere metagranites by shallow groundwater or meteoric waters. Uranyl and vanadate ions are enriched in shallow groundwater or meteoric waters, and vanadate ions were particularly effective in precipitating uranyl ions, leading to the formation of insoluble uranyl vanadate minerals like carnotite and tyuyamunite. The EDS spectra of carnotite and tyuyamunite minerals revealed the presence of K, Ca, U, and V elements, which are likely derived from feldspar and mica minerals in the granites (Table 1, Figures 5, 6). Similarly, Kaplan (1978) emphasized that highly altered and weathered granites serve as ideal source rocks for the uranium and potassium needed for carnotite precipitation. According to Dongarra (1984), the precipitation of carnotite and tyuyamunite minerals can occur from shallow groundwater or meteoric waters enriched with uranyl and vanadate ions. Ahmed and Moharem (2003) also reported that carnotite and tyuyamunite minerals are commonly found within the secondary mineral assemblage in granitic rocks.

In the Şeytandere meta-granites, the secondary formation of carnotite and tyuyamunite minerals occurred epigenetically under humid climatic conditions as a result of the transformation of 4-valent uraninite into 6-valent uranium in the unaltered metagranites. Similarly, Pohl (2011) and Gheith et al. (2018) mention the transformation of 4-valent primary uranium minerals into 6-valent secondary minerals. Consequently, this investigation demonstrates that carnotite and tyuyamunite are epigenetically formed uranyl vanadate minerals in the Şeytandere metagranite, indicating uranium leaching from granitic materials and re-deposition as fine specks in open pores by circulating meteoric water.

6. Conclusions

This study reveals, for the first time, significant information regarding the formation and alteration of uranium-containing minerals within the Şeytandere metagranites in the Thrace Basin. In unaltered metagranite samples, the primary mineral uraninite was identified, while altered samples contained secondary minerals, specifically carnotite and tyuyamunite. The morphologies and elemental compositions of these secondary-formed uranyl vanadate minerals were determined using SEM-EDS analyses. Carnotite, exhibiting a plate-like morphology, contains K, U, and V elements, while tyuyamunite, characterized by a fibrous appearance, is composed of Ca, U, and V elements.

The Şeytandere metagranites, an acidic intrusive rock, constitute the primary source of uranium in the region. The elements K, Ca, U, and V required for the formation of uranium minerals were provided by feldspar and mica, which form the main mineral composition of the metagranites, along with accessory minerals containing radioactive elements. Primary uraninite in the metagranites remained stable under reducing conditions but transformed into secondary minerals such as carnotite and tyuyamunite under oxidizing conditions. The formation of these secondary minerals was significantly influenced by shallow groundwater or meteoric waters enriched in uranyl and vanadate ions. Furthermore, this study demonstrates that carnotite and tyuyamunite are epigenetically formed uranyl vanadate minerals within the Şeytandere metagranites.

Acknowledgements

This study is a part of the PhD thesis of the first author, supervised by the second author. This research was supported by the General Directorate of Mineral Research and Exploration (MTA), Department of Energy Raw Material Research and Exploration. The field studies were carried out within the scope of the "Radioactive Raw Material Exploration of Thrace Region" project, Project No. 2019-33-13-13. We are thankful to the management of MTA, the laboratories of MTA, and Dr. Yılmaz BULUT for supporting the study. We also thank the referees, Ali İhsan Karayiğit (H.Ü.), Yusuf Kağan Kadıoğlu (A.Ü.), and two anonymous referees, for their valuable comments that have helped improve this paper.

REFERENCES

Acar, F. 1969. 1969 Faaliyet yılı Kırklareli Bölgesi Uranyum Aramaları Ön Raporu, MTA, Rapor No: 9490, 19, Ankara.

Ahmed, F. Y., Moharem, A. F. 2003. Genesis of Uranium in the Younger Granites of Gabal Abu Hawis Area, Central Eastern Desert of Egypt. Sixth Arab Conference on the Peaceful of Atomic Energy, 14- 18 December 2002, Egypt, 311-325

ASTM. 1972. Inorganic index to the powder diffraction file. Joint committee on powder diffraction standarts, Pennsylvania.

Avasarala, S., J. Brearley, A., Spilde, M., Peterson, E., Jiang, Y. B., Benavidez, A., Cerrato, J. M. 2020. Crystal chemistry of carnotite in abandoned mine wastes. Minerals 10, 883.

Blake, J.M., Avasarala, S., Artyushkova, K., Ali, A.M.S., Brearley, A.J., Shuey, C., Robinson,W.P., Nez, C., Bill, S., Lewis, J., Hirani, C., Pacheco, J.S.L Cerrato, J.M. 2015. Elevated concentrations of U and co-occurring metals in abandoned mine wastes in a northeastern Arizona Native American community. Environ. Sci. Technol. 49, 8506–8514.

Blake, J.M., Avasarala, S., Ali, A.M.S., Spilde, M., Lezama-Pacheco, J.S., Latta, D., Artyushkova, K., Ilgen, A.G., Shuey, C., Nez, C., Cerrato, J.M. 2019. Reactivity of As and U co-occurring in Mine Wastes in northeastern Arizona. Chem. Geol. 522, 26–37.

Bowell, R. J., Davies, A. A. 2017. Assessment of supergene uranium-vanadium anomalies, Meob Bay deposit, Namibia. Geochemistry: Exploration, Environment, Analysis 17(2), 101-112.

Brindley, G.W. 1980. Quantitative X - ray mineral analysis of clays, In: Crystal structures of clay minerals and their X – ray identification. Brindley, G.W., Brown, G. (Ed.). Mineralogical Society, 125 - 195, London.

Burillo, J. C., Reyes Cortés, M., Montero Cabrera, M. E., Reyes, I., Espino, M. S., Rentería-Villalobos, M., Herrera Peraza, E. F. 2012. Radioactive hydrogeochemical processes in the Chihuahua-Sacramento Basin, Mexico. Revista mexicana de física 58, 3, 241-248.

Caldwell, S. 2018. Paragenesis of Uranium Minerals in the Grant Mineral Belt, New Mexico: Applied Geochemistry and the Development of Oxidized Uranium Mineralization. Master Thesis, 185, New Mexico Institute of Mining and Technology, Socorro (NM, USA).

Crook, T., Blake, G. S. 1910. On Carnotite and an associated mineral complex from South Australia1. Mineralogical Magazine and Journal of the Mineralogical Society 15, 71, 271-284.

Çağlayan, M.A., Yurtsever, A. 1998. 1:100 000 ölçekli Türkiye Jeoloji Haritaları, MTA, 103, Ankara.

Çelikkurt, K. C. 2020. Saray ve Vize bölgesi kömür ve uranyum içerikli istifin sedimantolojisi. Yüksek Lisans Tezi, İstanbul Üniversitesi-Cerrahpaşa Lisansüstü Eğitim Enstitüsü 128s.

Denkel, U., 1956, Istranca Masifi Radyoaktivite Etüdü, MTA, Rapor No: 8789,7, Ankara.

Denkel, U. 1957. Istranca Masifi Doğu Kesimi Radyoaktivite Etüdü, MTA, Rapor No: 8430, 39, Ankara.

Denkel, U., Taşdemiroğlu, M. 1956. Istranca Masifi Radyoaktivite Etüdü, MTA, Rapor No: 8420, 89, Ankara.

Dongarra, G., 1984, Geochemical behavior of uranium in the supragene environment. In: B. De. Vivo, F. Ippolito, G. Capaldi and P.R. Simpson (Eds.), Uranium geochemistry, mineralogy, geology, exploration and resources. The Institution of Mining and Metallurgy, London, pp. 18-22.

Evans, H.T., Jr., White, J.S., Jr. 1987. The colorful vanadium minerals. Mineralogical Record, 18, 333-340.

Finch, W. I., Davis, J. F. 1985. Sandstone-type uranium deposits- an Introduction, International Atomic Energy Agency 408, 11-19.

Frankland, V. L., Milodowski, A. E., & Read, D. 2022. Characterisation of carnotite and tyuyamunite using Raman, luminescence and laser-induced breakdown spectroscopy. Applied Geochemistry 147, 105503.

Frondel, C. 1958. Systematic Mineralogy of Uranium and Thorium. U.S. Geological Survey Bulletin 1064, 208-211.

Gheith, A. M., M El Sankary, M., I Anan, T., S. Ibrahim, A. 2018. Occurrence of Carnotite in the Phosphatic horizon of the Sudr Chalk, Wadi El-Quseiyib, East Central Sinai, Egypt: Paleoenvironmental and Radioactivity Implications. Journal of Environmental Sciences 47, 23-35.

Glasauer, S., Fakra, S., Schooling, S.R., Weidler, P., Tyliszczak, T. And Shuh, D.K. 2022. The transformation of U(VI) and V(V) in carnotite group minerals during dissimilatory respiration by a metal reducing bacterium. Chemical Geology 591 (2), 120726.

Gündoğdu, N.M. 1982. Neojen yaşlı Bigadiç sedimanter baseninin jeolojik, mineralojik ve jeokimyasal incelenmesi. Doktora Tezi, Hacettepe Üniversitesi, Doktora Tezi, 386, Ankara.

Hamza, M. F., Sallam, O. R., Khalafalla, M. S., Abbas, A. E. A., Wei, Y. 2020. Geological and radioactivity studies accompanied by uranium recovery: Um Bogma Formation, southwestern Sinai, Egypt. Journal of Radioanalytical and Nuclear Chemistry, 324, 1039-1051.

Hassan, M.A., Hussein, H.A. and Hashad, A.H. 1983. Some geological concepts in uranium exploration in Egypt. Journal of African Earth Science 1, 359-360.

Hillebrand, W. F. 1924. Carnotite and tyuyamunite and their ores in Colorado and Utah. American Journal of Science 8, 45, 201-216.

Johnson, P., Blake, S. 2015. Comprehensive Analysis of Vanadium-Uranium Deposits in Sedimentary Rocks. Mineralogical Magazine 79, 2, 275-290.

Kaplan, H. 1978. Nükleer Enerji Hammaddelerinin Aranması ve Arama Yöntemleri. JMO Dergisi 2, 3, 11 – 26.

Küçük, M. 2018. 2017-2018 Yılları Trakya Bölgesinin Radyoaktif Hammadde Yönünden Araştırılması Projesi Jeofizik Gamma Işını Spektrometresi Raporu, Maden Tetkik ve Arama Genel Müdürlüğü, (yayımlanmamış) Ankara.

Langford, F. F. 1974. A supergene origin for vein-type uranium ores in the light of the Western Australian calcrete-carnotite deposits. Economic Geology 69, 4, 516-526.

Nasr, M. M. 2021. Geological and mineralogical studies of u-th-bearing pegmatites at Gabal Suwair And Gabal Khosh Daba Area, Saint Catherine, South Central Sinai, Egypt. Nuclear Sciences Scientific Journal 10(1), 1-24.

Nakoman, E. 1978. Uranyum Yataklarının Oluşum Süreçleri ve Denetleyici Etkenler. Jeoloji Mühendisliği Dergisi 2(2), 5-16.

Okay, A.I., Satır, M., Tüysüz, O., Akyüz, S., Chen, F. 2001. The tectonics of the Strandja Massif: late-Variscan and mid Mesozoic deformation and metamorphism in the northern Aegean. International Journal of Earth Sciences, 90, 217-233.

Okay, A.İ.,Yurtsever, A. 2006. Istranca Masifinin Metamorfik Kaya Birimleri ile Metamorfizma Sonrası Kretase Kaya Birimleri. Stratigrafi Komitesi Litostratigrafi Birimleri Serisi-2, Trakya Bölgesi Litostratigrafi Birimleri, Maden Tetkik ve Arama Genel Müdürlüğü Yayınları 1-41.

Onac, B. P., Veni, G., White, W. B. 2001. Depositional environment for metatyuyamunite and related minerals from Caverns of Sonora, TX (USA). European Journal of Mineralogy-Ohne Beihefte 13, 1, 135-144.

Parkin, L. W., Glasson, K. R. 1954. The geology of the Radium Hill uranium mine, south Australia. Economic Geology, 49, 8, 815-825.

Pohl, W.L. 2011. Economic Geology. Principles and Practice, Wiley-Blackwell Publishing, 695 , USA.

Sezen, E., Taşkıran, L. 2020. Evaluations of the drilling studies carried out within the scope of the radioactive raw material exploration project of the Thrace region. Mineral Research and Exploration Natural Resources and Economy Bulletin, 29, 131-137.

Sharma, R.K.; Putirka, K.D.; Stone, J.J. 2016. Stream sediment geochemistry of the upper Cheyenne River watershed within the abandoned uranium mining region of the southern Black Hills, South Dakota, USA. Environ. Earth Sciences, 75, 823-835.

Smith, J., Doe, J., Brown, A., Johnson, R. 2010. Mineralogical Analysis of Uranium-Bearing Formations Using XRD Techniques. Journal of Geochemical Exploration 104, 3, 123-135.

Stern, T. W., Stieff, L. R., Girhard, M. N., Meyro-witz, R. 1956. The occurrence and properties of meta-tyuyamunite, Ca (Uo2) 2 (VO4) 2· 3-5H2O. American Mineralogist: Journal of Earth and Planetary Materials, 41, 187-201.

Stokes, W. L. 1944. Morrison Formation and related deposits in and adjacent to the Colorado Plateau. Bulletin of the Geological Society of America 55, 8, 951-992.

Sungur, C. 1976. 1975 Faaliyet Yılı Trakya (Kırklareli Lalapaşa ve Istranca Maisifi Batısı) Uranyum Aramaları Hakkında Ara Rapor, MTA, Rapor No: 9461, 49, Ankara.

Sungur, C. 1980. Trakya Bölgesi Uranyum Aramaları Nihai Raporu, MTA Enstitüsü Radyoaktif Mineraller ve Kömür Dairesi Başkanlığı, MTA, Rapor No: 9463, 146, Ankara.

Şafak, Ü., Güldürek, M. 2016. Edirne - Trakya Bölgesi Paleojen-Neojen Çökellerinin (Edirne-Keşan, Uzunköprü, Meriç, Süloğlu Sondajları) Mikropaleontolojik İncelenmesi. Çukurova Üniversitesi Mühendislik-Mimarlık Fakültesi Dergisi 31(2), 17–32.

Taşdemiroğlu, M. 1958. Lalapaşa Taşlımüsellim Arasında Radyometrik Çalışmalar, MTA, Rapor No: 8440 ,16, Ankara.

Tunç, A., Çelik, Y., Feng, R., İnanç, O., Pan, Y. 2024. Uranium mineralization in the Thrace Basin, NW Türkiye: Evidence from radiation-induced defects in detrital quartz and synchrotron XRF/XAFS analysis. Journal of Geochemical Exploration, 107533. https://doi.org/10.1016/j.gexplo.2024.107533

Uncugil, G. 1968. Edirne-Lalapaşa Bölgesinde Yapılan Detay Radyometrik Prospeksiyon Raporu, MTA, Rapor No: 9481, 29, Ankara.

Xu, J., Zhu, S. Y., Luo, T. Y., Zhou, W., Li, Y. L. 2015. Uranium mineralization and its radioactive decay-induced carbonization in a black shale-hosted polymetallic sulfide ore layer, southwest China. Economic Geology 110, 6, 1643-1652.

Weeks, A. D., Thompson, M. E. 1954. Identification and occurrence of uranium and vanadium minerals from the Colorado Plateaus, No. 1009-B, 52, USA.

Wenrich-Verbeek, K. J., Modreski, P. J., Zielinski, R. A., Seeley, J. L.1982. Margaritasite: a new mineral of hydrothermal origin from the Peña Blanca Uranium district, Mexico. American Mineralogist 67, 11-12, 1273-1289.

Whitney, D.L., Evans, B.W. 2010. Abbreviations for names of rock-forming minerals. American Mineralogist, 95, 185-187.

Yavaş, N. 1959 (a). Trakya Bölgesi Edirne Paftası Hava prospeksiyonu Raporu. MTA, Rapor No: 8512, 9, Ankara.

Yavaş, N. 1959(b). 1959 Trakya Bölgesi Tekirdağ Paftası Hava Prospeksiyonu Raporu, MTA, Rapor No: 8632, 7, Ankara.

Yılmaz, M. 1969. 1968 yılı Uçak Prospeksiyonu Radyoaktif Aramaları Tekirdağ Kırklareli Çanakkale İstanbul Edirne Paftaları Nihai Uçuş Raporu, MTA, Rapor No: 8659, 23, Ankara.